

ECRH assisted plasma start-up with toroidally inclined launch: multi-machine comparison and perspectives for ITER

J. Stober¹, G.L. Jackson², E. Ascasibar³, Y.-S. Bae⁴, J. Bucalossi⁵, A. Cappa³, T. Casper⁶, M.-H. Cho⁷, Y. Gribov⁶, G. Granucci⁸, K. Hanada⁹, J. Hobirk¹, A.W. Hyatt², S. Ide¹⁰, J.-H. Jeong⁷, M. Joung⁴, T. Luce², T. Lunt¹, W. Namkung⁷, S.-I. Park⁷, P.A. Politzer², J. Schweinzer¹, A.C.C. Sips¹¹, the ASDEX Upgrade team¹, the TJ-II team³ and the ITPA "Integrated Operations Scenarios" group members and experts

¹ Max-Planck-Institut für Plasmaphysik, EURATOM-Association, Garching, Germany

² General Atomics, PO Box 85608, San Diego, CA 92186-5608, USA

³ Laboratorio Nacional de Fusión, Asociación EURATOM/CIEMAT, 28040, Madrid, Spain

⁴ National Fusion Research Institute, Gwahangno 113, Yuseong-gu, Daejeon 305-333, Korea

⁵ Association Euratom-CEA, Cadarache, F-13108 St. Paul-lez-Durance, France

⁶ ITER Organisation, Route de Vinon sur Verdon, F-13115 St. Paul-lez-Durance, France

⁷ Pohang University of Science and Technology, San 31, Hyoja-dong, Nam-gu, Pohang 790-784, Korea

⁸ Associazione Euratom-ENEA sulla Fusione, IFP-CNR, Via R. Cozzi 53, 20125 Milano, Italy

⁹ RIAM, Kyushu University, RIAM, Kasuga, Fukuoka, 816-8580 Japan

¹⁰ Japan Atomic Energy Agency, 801-1, Mukouyama, Naka, Ibaraki-ken, 311-0193 Japan

¹¹ EFDA JET, Culham Science Centre, Abingdon, OX14 3DB, UK

e-mail: Joerg.Stober@ipp.mpg.de

Abstract. ECRH assisted plasma break down is foreseen with full and half magnetic field in ITER. As reported earlier, the corresponding O1- and X2-schemes have been successfully used for pre-ionisation and breakdown assist in present day devices. This contribution reports on common experiments studying the effect of toroidal inclination of the ECR beam, which is $\geq 20^\circ$ in ITER. All devices could demonstrate successful breakdown assist also for this case, although in some experiments the necessary power was almost a factor of two higher compared to perpendicular launch. Differences between the devices with regard to the required power and vertical field are discussed and analysed. In contrast to most of these experiments, ITER will build up loop voltage prior to the formation of the field null due to the strong shielding by the vessel. Possible consequences of this difference are discussed.

1. Introduction

The superconducting solenoid and the thick vessel walls limit the available toroidal electrical field for plasma breakdown on ITER well below the values used in most of the operating Tokamaks. Although experiments on JET [1], DIII-D [2] and Tore Supra (TS) [3] show that an ohmic plasma start-up with the electrical field value of ITER (0.3 V/m) is marginally possible, assist of plasma breakdown by ECRH is highly desirable for ITER to increase the operational margin. To achieve initial plasma breakdown, ECRH can either create a low temperature plasma prior to the application of a loop voltage or in the presence of a loop voltage it may relax the Paschen-Criterion by additional acceleration of an otherwise sub-critical electron distribution [4]. In the subsequent current formation phase, when closed flux surfaces form and the electron temperature rises, ECR heating of the electrons can facilitate the sustainment of the breakdown through the radiation barrier when light impurities are ionized and radiate a significant fraction of the ohmic heating power. ECRH assist has already been investigated previously by the ITPA Steady-State-Operation group [1] and satisfactory results have been obtained for the fundamental and 2nd harmonic resonances. As explained below the optimum polarisations is O-mode in case of the fundamental resonance (O1) and X-mode for the second harmonic (X2). Mean-

while, KSTAR has used ECRH (X2) assist to break down its first plasmas [5]. Most of these results were performed with ECRH launched perpendicular to the magnetic field. Experiments with an inclined X2 scheme on DIII-D initially did not achieve sustained breakdown for an toroidal inclination of 20° degrees [6], the minimum value foreseen for ITER. In contrast to similar experiments with O1 on TS [3] and JT-60U [7], which could successfully breakdown with low voltage and large toroidal angles. To clarify the effect on toroidal inclination, the new ITPA Integrated-Operational-Scenarios group initiated a continuation of the joint experiments with the participation of the Tokamaks AUG(X2), DIII-D(X2), FTU(O1), KSTAR(X2), Tore Supra (O1, X2), and of the Stellarator TJ-II (X2). It should be noted that during the initial collision-less heating-phase of the pre-ionisation sequence, electron acceleration due to ECRH is dominantly perpendicular to the magnetic field [8], such that the large scale toroidal geometry does not play a significant role in this phase as long as no loop voltage is applied. Since in this study in all Tokamaks except FTU and TS the plasma was ionized by ECRH before the onset of the loop voltage, it is sensible to include as well Stellarators into a comparison of the conditions for the collision less heating phase.

2. Pre-ionisation with inclined ECRH

AUG, DIII-D [9], KSTAR, and TJ-II find that ECRH assisted breakdown in X2-mode is possible with a toroidal injection angle of 20° (or larger). FTU [10] obtains the same results for O1 in line with the older results from TS and JT-60U. These results indicate that a toroidal inclination of 20° as foreseen for ITER does in general not pose additional complications for plasma breakdown with ECRH, although some parameters need readjustment such as prefil and ECRH power. The results of the individual machines are detailed in table 1 for O1 and X2 heating. In all Tokamaks it was possible to reduce the necessary loop voltage by using ECRH assist. In most cases the toroidal \vec{E} -field on axis remained below the foreseen ITER value of 0.3 V/m. Exceptions are O1 experiments at FTU and X2 experiments at TS. FTU did not try lower voltage and in TS a non-optimised poloidal field null is regarded as reason for the unusual

Device	Ohmic			O1 perp			O1 inclined			X2 perp			X2 inclined			frequency
	\vec{E}_{min}	\vec{E}_{min}	P_{ECRH}	\vec{E}_{min}	P_{ECRH}	angle										
AUG	0.52	0.3	0.4				0.2	1.0		0.2	1.6	20				O1:105, X2:105,140
DIII-D	0.25[2] 0.43[6]	0.15[2]	0.8				0.21[6]	1.2		0.3[9]	0.6	23				O1:60, X2:60,110
FTU	1.3	0.41	0.8	0.69	0.4	20										140
JT-60U	1.5			0.26	0.4	20										118[7]
KSTAR	-						0.24	0.35		0.24	0.35	15				84 [5]
										0.29	0.24	20				110
TS	0.3	0.15	0.25	0.25	0.3	30	0.5	0.5		0.6	0.5	30				118[3,11]
T-10	0.44									0.28	0.45	21				140 [12]
QUEST		>3.0	0.06													8.2
TJ-II	-						-	0.08		-	0.14	>30				53.2

Table 1: optimized breakdown parameters (\vec{E} in V/m, P_{ECRH} in MW, angle in degree). Since \vec{E}_{Φ} varies in time during breakdown, \vec{E}_{min} corresponds to the minimum in a sequence of \vec{E}_{Φ} values, which are themselves the maxima of time-traces of \vec{E}_{Φ} of the analysed breakdown experiments. P_{ECRH} is the minimum power successfully tested with the cited value of \vec{E}_{min} . As discussed in the text below, these numbers are not the result of a multi-dimensional minimisation procedure, but rather singular points found in usually one-dimensional scans. Especially the loop voltages at inclined angles in AUG, DIII-D and FTU were not minimised. For a single device, the field null structure may vary between different entries (except KSTAR (84GHz) and TJ-II).

behaviour. As already reported in [1], a significant difference between the O1- and X2-schemes is the time delay between the start of the ECRH and a measurable plasma ionization (usually determined by H_α emission). With O1 an increase of this emission can be measured immediately after ECRH is switched on, independent of injection angle. With X2 the increase is delayed by several ms (during which the full ECRH power has to be absorbed by in-vessel components). This delay is dependent on the inclination angle, as demonstrated in figure 1 for TJ-II. As in DIII-D, AUG, and TS, the delay increases with the inclination angle. For KSTAR the situation is less clear. At least for the first ten

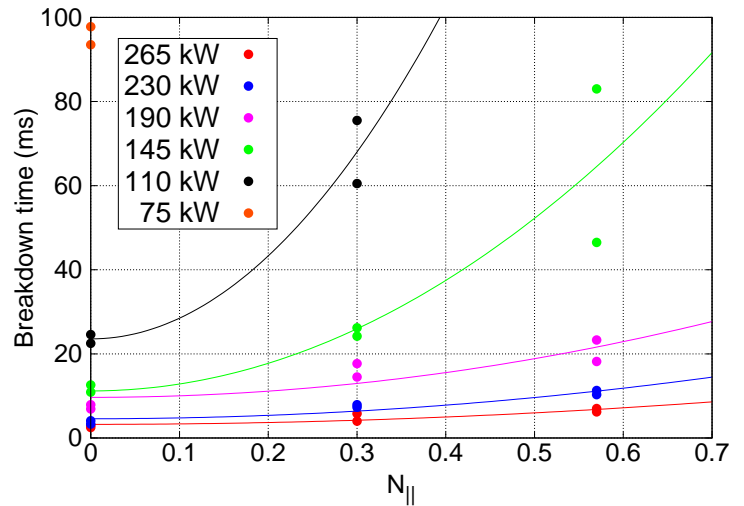


Figure 1: Effect of variation of the toroidal injection angle in TJ-II. Shown is the delay of the H_α rise after turning on the ECRH as function of $N_{||}$ for several ECRH powers (X2) with constant prefill (#23930-#23965). $N_{||} > 0.55$ corresponds to a toroidal injection angle $> 30^\circ$.

degrees the delay is slightly reduced in the case of 84 GHz [5]. To understand the difference between fundamental and 2nd harmonic resonance, the pre-ionisation process has to be described in some more detail: As an ECR-beam is injected into the neutral gas without a plasma, it is reflected, diffused, de-polarised and damped on in-vessel components and an undefined mixture of O-and X-mode polarisation will fill the whole vessel. The wave-field will still be highest in the injected beams, but also in other fractions of the vessel volume the intensity may be high depending on the injection angle, geometry of the first reflections, beam divergence and wall material. The latter determines the absorbed fraction per reflection (graphite: $\approx 1/20$, W: $\approx 1/500$ [13]140 GHz). A free electron will be accelerated perpendicular to the magnetic field since it dominantly absorbs on the X-mode polarisation. (The reason to inject the fundamental wave as O-mode is an X-mode cut-off at the low field side, which develops at very low densities, such that O-mode is necessary to assist sustainment of the breakdown through the radiation barrier later in the discharge.) By non-ionising collisions with the neutral gas the electron gains parallel momentum and moves to other regions of the plasma volume, where the \vec{E} field may be different. Since the magnetic field lines are not closed, it will finally be lost to the wall. The avalanche criterion basically is: do slow free electrons have in average the chance to accumulate so much ECRH power that they do create another (initially slow) electron by ionisation of a neutral atom before they hit the wall? The delay time which was observed corresponds in this picture to the time which is necessary to accelerate the first slow electrons to approximately 20 eV. For the fundamental resonance, absorption is very efficient even at low temperatures. Therefore acceleration is prompt. In contrast, X2 absorption vanishes for zero temperature and the heating rate is proportional to the electron perpendicular energy and the electric field. This leads to an exponential growth of the initially small (0.03 eV) electron energy in time and the electric field determines the exponential growth time. This model has been quantitatively analysed for DIII-D experiments in [8] and good agreement with experiment was found. Due to the exponential dependence on the electrical field, electrons are accelerated dominantly in regions of highest field. Results from T-10 [12] on the effect of beam focusing point in the same direction, i.e. the delay is significantly increased if the beam is defocused,

which strongly reduces the wave field. Potentially, the variation of the delay with beam inclination may also be related to a variation of the electrical field. For perpendicular launch reflections keep the beam center in the poloidal plane of injection, in this region the field is enlarged and a significant toroidal decay is expected. In case of toroidally inclined injection the enhancement by multiple reflections is reduced as is the maximum field strength. Stray-radiation detection in AUG supports this explanation as shown in fig. 2 for a toroidal angle scan of the ECRH beam in otherwise identical discharges. The

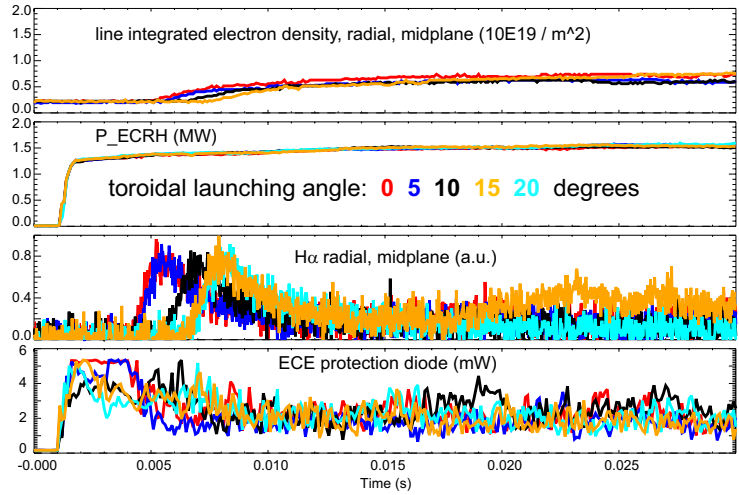


Figure 2: Scan of toroidal launching angle in AUG for 140 GHz X2-pre-ionisation at $B_t = 2.3$ T including effect on stray radiation. No significant differences were observed during current formation.

The above mentioned delay of the H_α -rise is clearly seen. The bottom trace shows the stray power entering the ECE optics, which is 22° degrees or 0.8 m toroidally separated from the next ECRH launcher which directs its beam (diameter during first path < 0.1 m) successively away from the diode as the toroidal inclination is increased. The diode signal at the onset of the ECRH is saturated for normal inclination and decreases with increasing inclination. As the H_α signal rises the stray radiation is reduced in all cases due to increased absorption on electrons with several eV of energy created by the avalanche process. Similar observations are made with sniffer probes in FTU. These results may suggest that strength of electrical field and the delay time are anti-correlated. The much higher absorption of X1 compared to X2 also has the effect that for X1 the field strength of the initial stray field is strong enough to breakdown a plasma along the whole resonance cylinder, whereas for X2 this is only the case in the vicinity of the points where the initial beams cross the resonance cylinder, typically close to the midplane. This can be nicely observed with fast visible cameras in several devices. For fundamental resonance heating in TS fig. 3 shows that the resonance cylinder lights up within the timing uncertainty, as the ECRH is switched on. In contrast fig. 4 shows that with X2 a plasma forms in the AUG midplane and extends upwards and downwards along the resonance with a vertical speed of 50-100 m/s. With $B_z/B_\Phi \approx 0.001$, the speed along field lines is 50-100 km/s, of the order of the generalised ion sound speed, which is 20 km/s for 10 eV electrons and cold ions .



Figure 3: O1 pre-ionisation in TS (TS-42249): Time traces of P_{ECRH} , I_p , \bar{n}_e (2 lines) and two frames from a CCD camera without filter, i.e. mostly H_α emission from [3]. Uncertainty of ECRH timing: ± 1 ms.

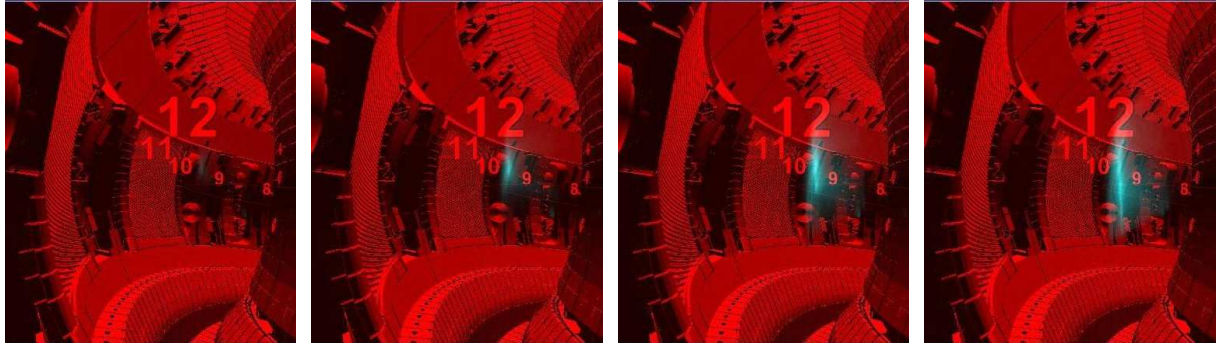


Figure 4: X2 pre-ionisation in AUG (#23177): 4 frames from a CCD camera without filter, i.e. mostly H_{α} emission (light blue) in front of visualised CAD-data (red, numbers correspond to sectors) at 9.1 ms, 10.1 ms, 11.2 ms, 12.2 ms. A total of 1.6 MW of ECRH was switched on (within 1 ms) at 0.0 ms, provided by four mid-plane launchers. At 12 ms the maximum of the H_{α} emission occurs. One launcher is visible in sector 8 but the intersection with the resonance cylinder is out of view. Therefore the light is probably emitted from a toroidal structure. The speed of its vertical extension is estimated to be 50-100 m/s.

The parameters shown in table 1 show significant inter-machine variation in terms of breakdown field and required ECRH power indicating the influence of additional parameters. In fact also the intra-machine variations are of similar relative size. Two major parameters are the prefil pressure and the structure of the poloidal field null, which are addressed in the next sections.

3. Prefil pressure

All devices find that ECRH assist allows to use significantly higher prefil pressures than for optimised low voltage breakdown. Systematic scans have been performed in TS, JT-60U, FTU, DIII-D (O1 and X2) and KSTAR. For O1 the possible range of prefil variation spans more than a factor of 4. For X2 at least a factor of 3 is found in DIII-D and KSTAR. Both experiments find that the upper limit increases with ECRH power. For constant ECRH power, the range for successful breakdown with X2 varies with the injection angle. This is the reason for the initially negative results in DIII-D for X2-breakdown with large toroidal launching angles as explained in [9]. Following the discussion at the end of the previous section it is most likely that for X2 the pressure-range narrows with increasing toroidal angle as the collisionality condition has to be met more accurately, if the local electric field is reduced by a toroidal inclination of the beam. For O1, FTU finds that 20° degree inclined injection widens the usable pressure range.

4. Field null

The issue of details of the field null seems to be especially crucial for X2-heating, as found in TS, where O1 experiments were performed prior to X2 experiments. Also DIII-D, TS, KSTAR and AUG find strong effects, if P_{ECRH} is close to the threshold. Ideally the poloidal field would be zero in the whole vessel during pre-ionisation and the electrons would only drift vertically with the $\nabla B \times B$ drift. In reality, a finite vertical field remains even in the plasma center such that parallel velocities have a non-zero projection in vertical direction which usually exceeds the $\nabla B \times B$ drift by about one order of magnitude. Additionally, non-zero radial field components exist as well, such that the corresponding projection of v_{\parallel} can move the electron radially. The 2-D patterns of B_R and B_z determine the poloidal field-null structure. It determines the connection lengths to the wall, which should be large. As found in DIII-D, it is also beneficial if the projected field lines are vertical in the vicinity of the resonance cylinder, i.e. $B_z \gg B_R$ in this region [14] as shown in figure 5. This makes fast electrons stay longer close to the resonance

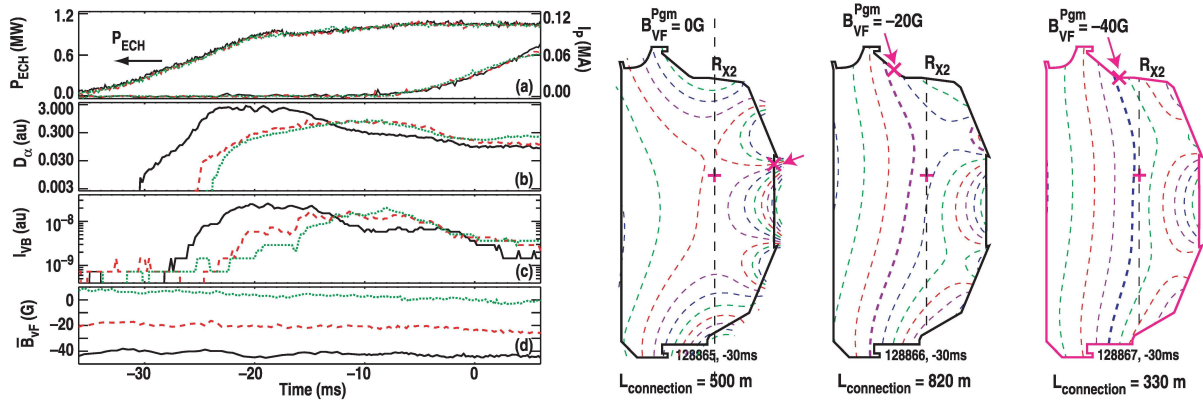


Figure 5: Pre-ionisation in DIII-D, scan of vertical field using a slow ECRH power ramp and corresponding poloidal flux surfaces. (From [14], figures 13 and 14, with permission of G.L. Jackson.)

such that the ECRH beam is absorbed more efficiently. In DIII-D, configurations with the lowest B_z have $B_R \approx B_z$. It can be seen that in this case an additional vertical magnetic field of ≈ 5 mT facilitates pre-ionisation although it reduces the connection length. The value of such an additional field depends on the initial field-null structure. TS and KSTAR find optimum additional $|B_z| < 2$ mT. For AUG, two field nulls have been used accidentally. In 2008 a very large null has been used with $B_{pol} < 2$ mT, but nevertheless a perfectly vertical initial ECR plasma (fig. 4). In 2009 the area where $B_{pol} < 2$ mT was much smaller and the initial ECR plasma was bent away from the resonance cylinder. In the latter case additional B_z helped. These AUG results indicate that an additional B_z is not always necessary to align the initial plasma with the resonance cylinder, but optimization of the field null may be important too. We note here that also for the spherical tokamak QUEST ECRH assisted breakdown is reported with non-zero vertical field. Since the resonance is located in this case essentially on the inner heat shield, it is not clear that the process is directly comparable to the other Tokamaks where the initial plasma generation is well separated from the walls.

5. Current formation and impurity burn-through

As the loop voltage is applied in Tokamaks, a toroidal current rises, which may lead to the formation of closed flux surfaces. Initially, it has to form in a location where it can grow until it is strong enough to influence its position by FB-control with the poloidal field coils. In this phase of FF-control the value of B_z is also crucial. Since \dot{B}_z is limited, the values of B_z during pre-ionisation and during current formation are strongly coupled and it is hard to say which one determines the optimum. It is usually found that the current does not form at the ECRH resonance. On AUG with ECRH the current forms close to the outboard limiters but without ECRH it forms close to the inner heat shield although poloidal field currents are programmed to be identical and the resonance is closer to the inboard side. The difference may be due to different vessel currents, since the loop voltage is different in both cases. These vessel currents are hard to determine, which prevented so far an inter-machine comparison. In fact, in DIII-D the current forms on the in-board side in both cases and it would be definitely interesting to understand the differences between both devices. As mentioned above, during the ionisation of light impurities too much power may be radiated that the breakdown is not sustained. Obviously this radiation is related to the impurity densities, such that machine condition plays an important role for this phase. In AUG it has been found that the current ramp-rate is significantly higher in the boronised machine as compared to the unboronised W-coated machine. The effect is most likely due to the remotely deposited Boron which acts as a getter for light impurities. On AUG

and DIII-D, ECRH has also been used successfully after ohmic breakdown to burn through this radiation barrier (in AUG from 20ms until 70ms after start of U_{loop} -ramp).

6. Minimum power and size scaling

Usually it is found that more ECRH power widens the operational range for breakdown for essentially all relevant parameters. Inversely, this means that all parameters have to be adjusted simultaneously to find the absolute minimum of ECRH power for a specific loop voltage and even when doing so, the result will depend severely on wall conditions. Some partial parameter scans were done, but no machine has systematically tried to reduce the required ECRH power to the bare minimum. Especially for the field null this is a high dimensional minimisation procedure. Still, it is noted that TS and JT-60U which differ a factor of 2 in minor radius find approximately the same values of required ECRH power (< 0.4 MW) to obtain breakdown with O1 for a toroidal \vec{E} -field of 0.25 V/m. It is also noted that KSTAR, driven by limited ECRH power in the early stage of the machine, found a parameter range for X2 assisted plasma breakdown, with ECRH power well below values found on DIII-D and AUG, indicating some margin in the results presented here. It is also noted that the machines using X2 assist in these joint experiments are of similar size, such that no conclusions on a size scaling can be drawn.

7. Consequences for ITER

In summary it is found that the toroidal inclination of the beams poses no principal problem to ECRH assisted breakdown, but the required ECRH power may be higher, especially with X2. Unfortunately it is difficult to transfer the results on ECRH assist directly to ITER, since in ITER the field null is only formed when a significant fraction of the loop voltage is already applied [15], because the vessel screening times are large (see figure 6). This is in contrast to the performed experiments for which the loop voltage was virtually zero (except FTU and TS, see below), in order to separate the pre-ionisation phase from the current formation phase. In the case of full magnetic field, (O1) ionisation by ECRH takes place along the whole resonance cylinder, such that it is expected that in the presence of a significant loop voltage ECRH assist may initiate the breakdown and will significantly reduce the necessary loop voltage. The experiments in FTU, which use ECRH only after application of the loop voltage point in this direction, since a significant reduction of the loop voltage is achieved.

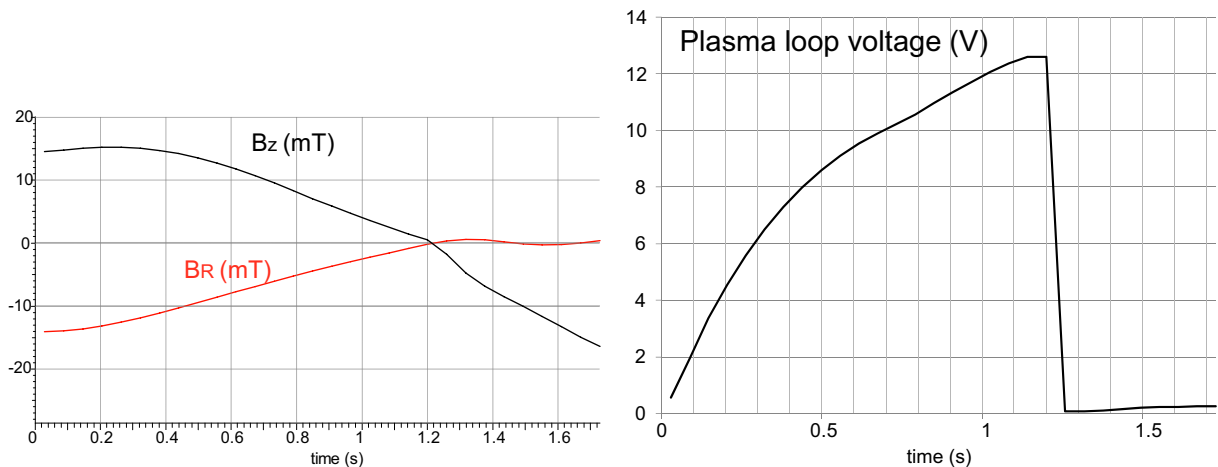


Figure 6: Estimated wave forms for B_z , B_R and U_{loop} during breakdown in ITER in the center of the breakdown region for a scenario with full field, fully charged central solenoid and initial current formation on low field side. From [15], figures 6-5, 6-6 and 6-13. Breakdown occurs at 1.2 s.

Figure 7 shows the FTU results. With ECRH, breakdown is possible at lower loop voltage. The delay of current and temperature rise with respect to the start of the ECRH may be due to the time evolution of the field null which moves radially outward toward the ECRH resonance. This effect which has a strong similarity to the ITER plans will be analysed in future experiments at FTU. In TS, the loop voltage and a

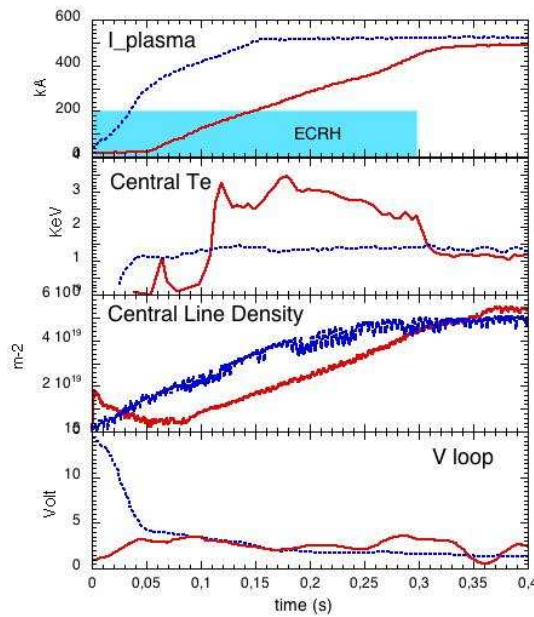


Figure 7: Breakdown in FTU ohmic (blue) and with ECRH assist (red). Shown are plasma current, central T_e , central line averaged density and loop voltage. The blue shaded area represents the wave form of the ECRH power (400 kW) in case of ECRH assist.

good field null are applied before the ECRH. In that case (fig. 3) the ECRH triggers plasma breakdown and current rise. For half magnetic field (X2) the beneficial effect of ECRH assist may be significantly smaller, since ionisation with ECRH requires that the electrons stay long enough in regions with high ECRH field, from which they are drawn away by the non-zero loop voltage. This needs to be addressed by dedicated future experiments.

References

- [1] SIPS, A. C. C. et al., Nucl. Fusion **49** (2009) 085015.
- [2] LLOYD, B. et al., Nucl. Fusion **31** (1991) 2031.
- [3] BUCALOSSI, J. et al., Electron cyclotron resonance heating assisted plasma start-up in the Tore Supra tokamak, in *Preprints of the 22nd IAEA Conference Fusion Energy, Geneva, Switzerland, October 2010*, volume <http://www-pub.iaea.org/MTCD/Meetings/fec2008pp.asp>, pages ex_p6–12.pdf.
- [4] LLOYD, B. et al., Plasma Phys. Controlled Fusion **38** (1996) 1627.
- [5] BAE, Y. S. et al., Nucl. Fusion **49** (2009) 022001.
- [6] JACKSON, G. L. et al., Nucl. Fusion **49** (2009) 115027.
- [7] KAJIWARA, K. et al., Nucl. Fusion **45** (2005) 694.
- [8] JACKSON, G. L. et al., Nucl. Fusion **47** (2007) 257.
- [9] JACKSON, G. L. et al., Experiments simulating ITER Rampdown and startup scenarios in the DIII-D tokamak, in *Europhysics Conference Abstracts (CD-ROM, Proc. of the 36th EPS Conference on Plasma Physics, Sofia, 2009)*, edited by MATEEV, M. et al., volume 33E, pages P–4.139, Geneva, 2009, EPS.
- [10] GRANUCCI, G. et al., ECRH assisted start-up studies and experiments on FTU, in *Europhysics Conference Abstracts (CD-ROM, Proc. of the 36th EPS Conference on Plasma Physics, Sofia, 2009)*, edited by MATEEV, M. et al., volume 33E, pages P–1.164, Geneva, 2009, EPS.
- [11] BUCALOSSI, J. et al., Nucl. Fusion **48** (2008) 054005.
- [12] KIRNEVA, N. A. et al., Plasma start-up optimisation with 2nd harmonic ECR pre-ionization in T-10 tokamak, in *Europhysics Conference Abstracts (CD-ROM, Proc. of the 34th EPS Conference on Plasma Physics, Warsaw, 2007)*, edited by GASIOR, P. et al., volume 31F, pages P–1.164, Geneva, 2007, EPS.
- [13] KASPAREK, W. et al., Int. J. Infrared Millimeter Waves **22** (2001) 1695.
- [14] JACKSON, G. L. et al., Fusion Sci. Tech. **57** (2010) 27.
- [15] KAVIN, A. A. et al., Study of Plasma Start up, ITER Contract No. ITER/CT/09/430000003, 2nd Intermediate Report, Study of plasma initiation using TRANSMAX code: ITER design "baseline 2010", Technical Report ITER, private communication, 2010.